

## Spatial layout of forecasted extreme temperatures in the city of Murcia (Spain)

L. Bañon and E. Hernandez

AEMET Regional Office in Murcia, Av. Libertad, 11, 30107 Murcia

Received: 6-I-2012 – Accepted: 17-I-2013 – **Original version**

Correspondence to: lbanonp@aemet.es

### Abstract

*The extremely warm summer of 2003 across Europe encouraged the development of a Spanish “Heat Wave Warning System”. The health authorities issued extreme temperature warnings to the population using extreme temperatures that were forecasted for the provincial capitals. The forecast of extreme temperatures is created by means of the post-processing of ECMWF EPS. For the Murcia region, the heat wave warnings are generated using extreme temperatures from the Murcia observatory, which is located in the suburbs of the city of Murcia. However, under this warning system, some uncertainties were raised regarding the difference between temperatures in the city and in rural areas. Therefore we designed a thermometric network to cover both areas. We analysed the differential behaviour of extreme temperatures between urban and rural areas, as a function of the sky view factor (SVF). We carried out an exercise for forecasting extreme temperatures in each part of the city of Murcia, based on the SVF and meteorological parameters. The final objective is to design an automated process that incorporates forecasted meteorological variables and SVF values, in order to generate thermometric maps, which will show the spatial layout of forecasted extreme temperatures in the city of Murcia.*

**Key words:** forecasted urban extreme temperatures, sky view factor, urban heat island, urban cool island

### 1 Introduction

The European heat waves in the Northern Hemispheric summer of 2003 were responsible for the deaths of tens of thousands of people (WMO, 2007; Robine et al., 2007). As a result, in 2004, the health authorities and the Spanish Meteorological Agency (AEMET) developed a National Plan of preventive actions against the negative health effects of excessive temperatures (Orden PRE/1518/2004). In this Plan, AEMET provides the forecasted extreme temperatures at meteorological observatories in the provincial capitals for the following five days. Thus, the health authorities can establish a number of preventive measures when the forecasted extreme temperatures surpass the specified thresholds.

These thresholds were established by means of the analysis of the correlation between extreme temperatures and recorded morbidity and mortality rates. For the Murcia region, these thresholds were chosen according to the 95th per-

centile of extreme summer temperatures from the meteorological observatory of Murcia. These threshold values are 38°C and 22°C.

The forecasted extreme temperature values, provided by AEMET to the Plan, are based on the Ensemble Prediction System (EPS) median from the ECMWF (European Centre for Medium-Range Weather Forecasts) value in the nearest meteorological observatory for each provincial capital.

As a rule, urban climate behaviour differs from rural climate (López-Gómez et al., 1991; Eliasson, 1996; de Stefens et al., 2001). Therefore, the health authorities questioned whether the Plan had underestimated the situations in which forecasted extreme temperatures had not reached the thresholds in rural areas, but had managed to do so in the city, meaning a risk for its citizens.

From these uncertainties raised, a research project was developed, starting with the design of a thermometric urban network in the city of Murcia. Afterwards, the observed



**Figure 1.** Map showing the location of the city of Murcia.

temperature differences between urban and rural areas were studied, obtaining a functional relationship with urban parameters. In order to extend the extreme temperature predictions outlined in the Plan to different points of the city of Murcia, an adjustment was made using Model Output Statistics (MOS) between the differences observed and the urban and predicted meteorological variables. These relationships made it possible to predict the spatial distribution of extreme temperatures in the city of Murcia by means of predicted meteorological data, which were developed by the EPS in the Murcia observatory.

## 2 Data and Methodology

### 2.1 Study area

The study area of this project was the city of Murcia, the capital of the Murcia region, which is located in the southeast of Spain (Figure 1). The city of Murcia has a population of over 400,000 people and lies in a valley 35 km from the Mediterranean Sea. Its average altitude is 50 m and the city is largely flat, crossed by the Segura River. The meteorological observatory is situated 4 km northwest of the city centre, in a rural area.

### 2.2 Sky View Factor (SVF)

The differences in extreme temperatures between the city and rural areas are influenced by both meteorological and urban parameters. Some urban climate research has demonstrated the influence of urban parameters on extreme temperatures, such as traffic density, urban layout, distance to sources of humidity, material reflectivity and so on (Oke, 1988; Lindberg et al., 2003; Fernández et al., 2004).



**Figure 2.** Fisheye image. Unger (2009).

Of these urban parameters, the sky view factor (SVF) is one of the most important ones, according to Steyn (1980), Eliasson (1996), Unger (2004) and Oke (2007). With reference to Unger (2004), the intra-urban distribution of the temperature excess is largely dependent on local surface characteristics, such as geometry: building heights ( $H$ ), street (canyon) width or spaces between buildings ( $W$ ). The  $H/W$  ratio describes how densely buildings are spaced with respect to their height. However, a more appropriate measure of radiation geometry of a given site is its SVF. Moreover, the SVF is one of the main causes of urban heat islands (Souza et al., 2003).

The SVF is a parameter that indicates the relationship between the visible area of the sky and the area covered by urban structures (Souza et al., 2003). The SVF is a dimensionless measurement between 0 and 1, representing totally obstructed and free spaces, respectively (Unger, 2004). Taking a point of the urban surface, one part of the radiation from the point is absorbed by the surfaces around the point (buildings, trees, etc.) and the remaining part is directed to the sky. The measurement of this part is defined as the SVF.

There are some methods aimed at estimating or calculating the SVF in an urban environment, such as scale models, manual and computer-based evaluation of fisheye photos (Figure 2), computer evaluation of a 3D database describing surface geometric elements, etc. (Unger, 2009).

In this project, the SVF in every point of the city of Murcia was calculated using a method of computer evaluation of a 3D database describing surface geometric elements. The SVF was estimated by means of the sky view factor module implemented in SAGA (System for Automated Geoscientific Analyses) (Olaya, 2004), which is a geographical information system (GIS) software. For the SVF estimation, we used a layer of polygons for the streets in the city of Murcia, where the height of buildings was one of the attributes found in the table corresponding to this layer. The polygon layer was transformed to a grid (one metre cell size), in which the

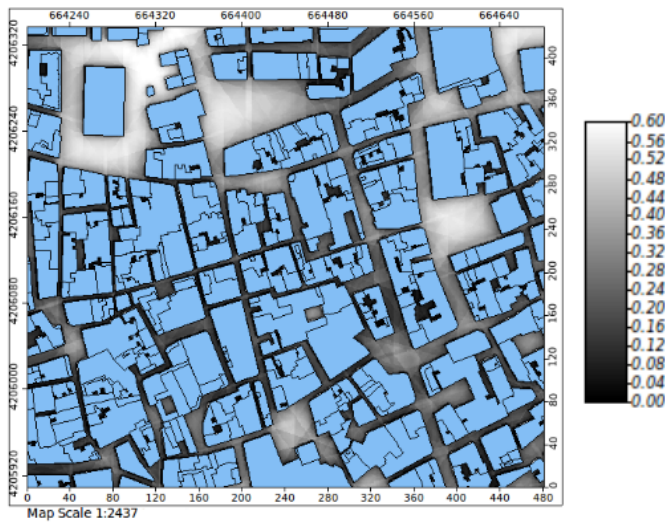


**Figure 3.** SVF values obtained in the streets of the city of Murcia using SAGA.

SVF was calculated. Thus, the SVF in every square metre of the city was obtained (Figure 3).

### 2.3 Thermometric network

In order to study the thermal patterns of the city of Murcia, a thermometric network was designed in the city as well as in rural areas during the summer of 2010, from 25 June to 30 September (98 days). The temperature sensors were installed in some points of the city, in accordance with the World Meteorological Organization (WMO) assessments (Oke, 2004).

The sensors used were MicroLITE from Dostmann-Electronic, which have negative temperature coefficient thermistors (NTC) inside. They include a small data logger for monitoring and recording temperatures. The sensors took and recorded measurements every ten minutes. We chose these devices due to the simplicity of taking and recording measurements, which can be downloaded to the computer for analysing recorded data.

Sensors were installed 3 m above the ground and were protected by weather shelters. Five sensors were installed on the city's lampposts and a sixth one was classed as the reference sensor, which was installed in the meteorological garden at Murcia observatory, in order to study the differential behaviour of extreme temperatures between urban and rural areas.

Due to the reduced number of sensors used to design the thermometric network, it was a difficult task to identify the dependence of urban parameters on the differences in temperature between urban and rural areas. Therefore, we focused on the SVF in order to analyse this dependence, as it is one of the main urban parameters according to some research (Subsection 2.2). Therefore, the distribution of sensors in the

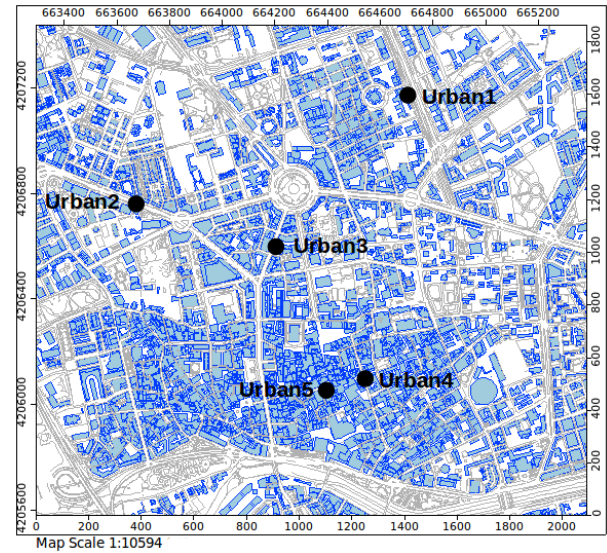


**Figure 4.** Map showing the distribution of sensors in the city of Murcia across the thermometric network. The sensor in the rural area was located 4 km northwest of the city centre.

city of Murcia (Figure 4) was chosen with the objective that sensors would cover a wide range of SVF values (Table 1) and for similar conditions in other urban parameters. In addition, we made some transects in the city to ensure the representativeness of the recorded temperature measurements.

### 2.4 Analysis of the differential behaviour between urban and rural extreme temperatures. Regression models

In order to analyse temperature behaviour in the city, the average hourly temperatures during the period in question were obtained, taken at each one of the network's locations. Afterwards, the differences by the hour between each urban and rural location were calculated.

The means of the maximum daily temperatures ( $T_{mean.max}$ ) obtained during the period were also calculated, as were the means of the minimum daily temperatures ( $T_{mean.min}$ ). Afterwards, we worked out the mean maximum temperature differences,  $\Delta T_{mean.max}(urban_k - rural)$ , between each urban location of the network ( $urban_{k=1-5}$ , see Table 1) and the rural area. Moreover, we worked out the same for minimum temperatures,  $\Delta T_{mean.min}(urban_k - rural)$ . Subsequently, some linear adjustments between  $\Delta T_{mean.max}(urban_k - rural)$  with the corresponding SVF values of each  $urban_k$  location and between  $\Delta T_{mean.min}(urban_k - rural)$  and these SVF values were obtained.

Given that the aim of the project was to extend the extreme temperature predictions outlined in the Plan from the rural area to different points of the city of Murcia, the differences observed ( $\Delta T_{extremes}(urban_k - rural)_{observed}$ ),

**Table 1.** SVF values and street orientation of the sensor locations across the thermometric network.

	rural	urban <sub>1</sub>	urban <sub>2</sub>	urban <sub>3</sub>	urban <sub>4</sub>	urban <sub>5</sub>
SVF	0.84	0.67	0.52	0.34	0.21	0.07
Street orientation	-	N-S	E-W	NE-SW	SE-NW	E-W

where the *extremes* are both maximum and minimum, were adjusted, using predicted meteorological variables as well as the SVF. The exercise was a statistical interpretation of the numerical model outputs (Model Output Statistics, MOS). This method, developed by Glahn and Lowry (1972), is an objective weather forecasting technique which consists of determining a statistical relationship between a predictand and variables forecast by a numerical model at some projection time. The chosen meteorological parameters were those predicted by a post-processing of EPS at the Murcia observatory, described in Table 2.

In the MOS exercise, for a given day the observed differences in extreme temperatures between each *urban<sub>k</sub>* location and the rural area,  $(\Delta T_{\text{extremes}}(\text{urban}_k - \text{rural}))_{\text{observed}}$ , were adjusted to the meteorological variables forecasted for this day on the previous day,  $(VRB_i)_{\text{simulated}}$ , (e.g.  $VRB_1$ : cloudiness,  $VRB_2$ : wind speed, etc.) and SVF values ( $SVF_k$ ). This adjustment is shown in Equation 1, where  $A_i$ ,  $B$  and  $C$  were the coefficients calculated in MOS.

$$(\Delta T_{\text{extremes}}(\text{urban}_k - \text{rural}))_{\text{observed}} = \sum_i A_i (VRB_i)_{\text{simulated}} + B(SVF_k) + C \quad (1)$$

We used R 2.7.0. (Becker et al., 1988) as the software for the development of forecasting models and for statistical calculations, and the generalized linear model (GLM) in order to estimate the connection between *urban-rural* extreme temperature differences and meteorological parameters and SVF.

Across the total measurement period, we chose 20 days of each month at random (60 days in total) to calculate forecasting models (MOS) and we checked the accuracy of the models obtained using the remaining 10 days of each month (control days). For this, some statistical data were calculated, such as the residual mean, the root-mean-square error (RMSE) and the bias.

## 2.5 Spatial layout of urban forecasted extreme temperatures. Thermometric maps.

In order to identify the spatial distribution of forecasted extreme temperatures in the city of Murcia, using Equation 1 we would obtain the differences in extreme temperatures with the rural environment for each one of the urban areas whose SVF are known. Accepting the prediction of extreme temperatures in the rural environment for the next day, developed during the post-processing of EPS within the Plan's

framework, we could approximate Equation 1 for the calculation of extreme temperature values to any point of the city, according to Equation 2.

$$T_{\text{extreme}}(\text{urban}_k) - T_{\text{extreme}}(\text{rural})_{\text{simulated}} = \sum_i A_i (VRB_i)_{\text{simulated}} + B(SVF_k) + C \quad (2)$$

In this way, the maximum and minimum temperature values in each point of the city where the SVF value is known could be obtained. Furthermore, some thermometric maps could be generated, which show the spatial layout of urban extreme temperatures.

## 3 Results and discussion

### 3.1 Results of the thermometric network

From the analysis of the differences in average hourly temperatures between urban and rural areas over the thermometric network period (Figure 5), we can highlight the following points.

The results reveal that the urban heat island effect (UHI) was more evident in locations with a lower SVF, changing from approximately 2°C for locations with low SVF values to less than 1.5°C for locations with high SVF values, as an average. This dependence was more pronounced at the end of the night, when the warming insulation in buildings disappeared, depending on their orientation. During the early hours of the night, the locations which were exposed to solar radiation in the evening showed a highlighted UHI effect (Oke et al., 1991; Cuadrat et al., 2005). The urban location of  $SVF = 0.52$  (*urban<sub>2</sub>*) is the best example of this effect, taking place from 7pm to midnight (Figure 5).

According to Figure 5, the differences between urban and rural areas remained constant or increased from midnight to sunrise, except at the *urban<sub>2</sub>* station ( $SVF = 0.52$ ), which showed a decreasing difference. This might be due to its proximity to a rural area located in the west of the city (see Figure 4), from where the nocturnal breeze came (Figure 6).

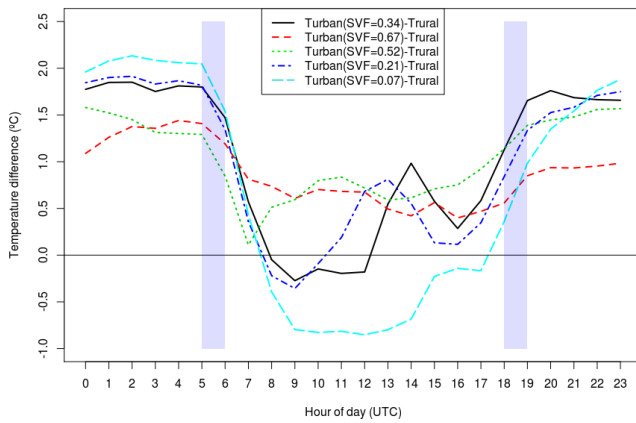
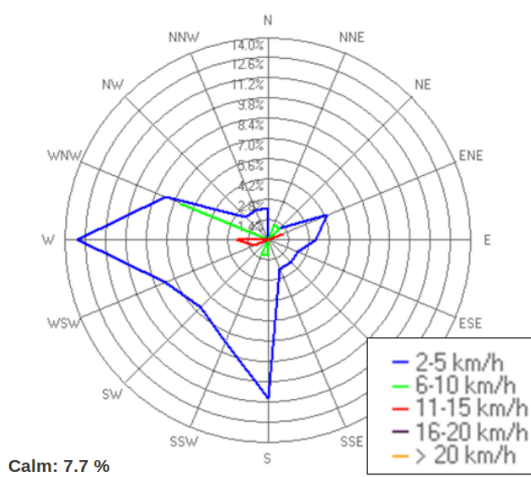
After sunrise, the rapid thermal increase in the rural area ( $SVF = 0.84$ ) kept the differences with urban locations to a minimum value. The urban locations which had received solar radiation from the early hours of the morning (high SVF values,  $SVF = 0.67$ , and streets with E-W orientation,  $SVF = 0.52$ ) stayed warmer than the rural area.

During the day, the urban locations with lower SVF values remained slightly cooler than the rural area (Cuadrat et al., 2005), a phenomenon known as the urban cool island



**Table 2.** Meteorological parameters for MOS.

Meteorological parameter	Units	Abbreviation
Maximum temperature	°C	$T_{max}$
Minimum temperature	°C	$T_{min}$
Wind speed at 00, 06, 12 and 18 UTC	km h <sup>-1</sup>	$Wind_{00UTC,06UTC,12UTC,18UTC}$
Cloudiness at 00, 06, 12 and 18 UTC	Tenths	$Cloud_{00UTC,06UTC,12UTC,18UTC}$

**Figure 5.** Evolution of the differences in average hourly temperatures between urban and rural areas over the thermometric network period. Columns in grey show the sunrise and sunset periods.**Figure 6.** Wind rose direction frequency at 07 UTC in Murcia observatory, during the network period.

effect (UCI). Locations with SVF values higher than approximately 0.4, which were more exposed to solar radiation, did not show this phenomenon. Moreover, the UCI effect disappeared as the solar radiation reached the street. Thus, in streets with a low SVF value and E-W or NW-SE orientation (see Table 2 and Figure 5), the UCI effect disappeared during the morning, while the effect disappeared during the evening in streets orientated towards the NE-SW, even with a higher SVF value (see Table 2 and Figure 5).

The differential behaviour between urban and rural temperatures when both of them were influenced by direct solar radiation ranged from 0.5 and 1°C. This might be due to the lower albedo in urban locations (Fortuniak, 2008).

## 3.2 Regression models

### 3.2.1 Minimum temperatures

From the analysis of the SVF effect on the mean minimum temperature differences between urban and rural areas,  $\Delta T_{mean.min}(urban_k - rural)$ , we noticed that the increase in SVF values produced a decrease in temperature differences, which was expected (UHI, Oke et al., 1991). The linear adjustment between mean minimum temperature differences and SVF ( $R^2 = 0.74$ ) is shown in Figure 7.

Once the dependence between *urban-rural* mean minimum temperature differences and SVF had been detected, we carried out an MOS exercise for the next day forecasted differences between urban and rural areas, based on the next day forecasted meteorological parameters and SVF. Considering the meteorological parameters (Table 2), as well as SVF values, we obtained the functional relationship and statistical data, detailed in Table 3.

$$\Delta T_{min}(urban - rural) = 2.19 - 0.03(Cloud_{00}) - 1.05(SVF) \quad (3)$$

From the meteorological parameters included in the MOS exercise (Equation 3), the cloudiness at 00 UTC was the only one which remained in the adjustment. The difference between overcast and clear skies produced a variation of 0.3°C in  $\Delta T_{min}(urban - rural)$ , since cloudiness reduces the effect of nocturnal irradiation, thereby decreasing the  $\Delta T_{min}(urban - rural)$ . The adjustment shown in Equation 3 can vary up to 1°C between locations with a high and low SVF.

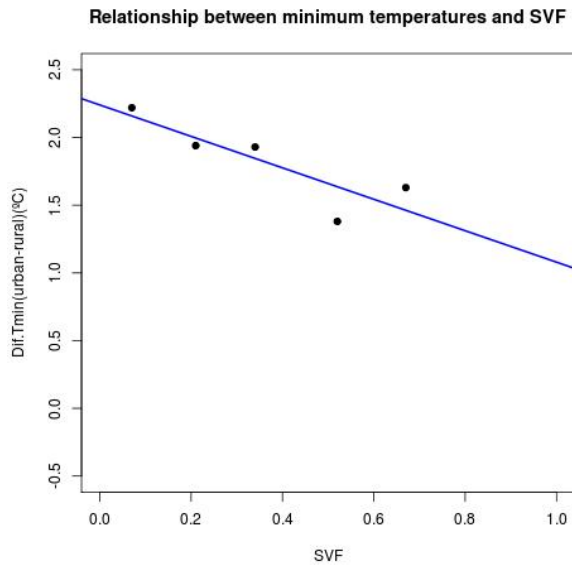


**Figure 7.** Regression of mean minimum temperature differences between each urban location and the rural area (SVF = 0.84) for SVF values.

**Table 3.** Statistical adjustment for the next day forecasted minimum temperature differences by MOS. Indicators of the statistical adjustment and verification process using control days.

Akaike Information Criterion (AIC)	425
Residual deviance (SCE)	78
Dispersion parameter ( $\phi$ )	0.31
VERIFICATION PROCESS (CONTROL DAYS)	
Residual mean	-0.18
Root-mean-square error (RMSE)	0.37
Bias	0.18

The results from the verification process of the model obtained (Equation 3) are shown in Table 3. These statistical data were calculated using the control days, according to Subsection 2.4.

### 3.2.2 Maximum temperatures

From the analysis of the SVF effect on the mean maximum temperature differences between urban and rural areas,  $\Delta T_{mean,max}(urban-rural)$  (Figure 8 left), we noticed that this adjustment was not representative ( $R^2=0.15$ ). Therefore, we proposed two alternative linear adjustments (Figure 8 right) between *urban-rural* mean maximum temperature differences and high and low SVF values, respectively. These approaches showed better linear adjustment ( $R^2 = 0.99$  and  $R^2 = 0.96$ ).

According to Figure 8 (right), the dependence between  $\Delta T_{mean,max}(urban-rural)$  and SVF low urban values ( $SVF \leq 0.33$ ) had grown, meaning that as the SVF values

**Table 4.** Statistical adjustment for the next day forecasted maximum temperature differences by MOS. Indicators of the statistical adjustment and verification process using the control days.

	SVF $\leq 0.33$	SVF $\geq 0.33$
AIC	263	202
SCE	48	32
$\phi$	0.33	0.22
VERIFICATION PROCESS (CONTROL DAYS)		
Residual mean	-0.05	0.00
RMSE	0.40	0.22
Bias	-0.05	0.00

increased, the urban area recorded higher differences. This behaviour could be explained by the fact that a small portion of the direct solar radiation reaches the narrow streets, leaving these areas cooler than the rural area (UCI). With an increase in SVF values, the direct solar radiation reaches the streets more easily. In general, the albedo in urban areas is lower than in rural ones, so the warming of the urban areas will be higher when compared to a rural environment, increasing the temperature differences between them.

For SVF high urban values ( $SVF \geq 0.33$ ), the direct solar radiation reaches the streets easily, decreasing the shaded areas. In this case, the effect of the wind speed predominates over the radiation effect. With the increase in SVF values, a higher wind speed is expected, which would tend to eliminate thermal superadiabatic gradients which can remain in poorly ventilated sunny streets. This phenomenon should explain the decreasing dependence between  $\Delta T_{mean,max}(urban-rural)$  and SVF high urban values.

Considering the next day forecasted meteorological parameters (Table 2), as well as SVF values, we obtained the functional relationship and statistical data, as outlined in Table 4. According to the two proposed linear adjustments, the next day forecasted maximum temperature differences (*urban-rural*) were adjusted for the locations with high and low SVF values.

$$SVF \leq 0.33 : \Delta T_{max}(urban-rural) = -0.58 - 0.04(Cloud_{12}) + 5.13(SVF) \quad (4)$$

$$SVF \geq 0.33 : \Delta T_{max}(urban-rural) = 1.93 - 0.09(Wind_{12}) - 1.84(SVF) \quad (5)$$

According to Equation 4, the cloudiness at 12 UTC was the only meteorological parameter which remained in the adjustment. Confirming the proposed adjustment for low values of SVF, the effect of cloudiness reduces the  $\Delta T_{max}(urban-rural)$  for locations with low and very low SVF values. The difference between overcast and clear skies would reduce the  $\Delta T_{max}(urban-rural)$  by  $0.4^\circ\text{C}$ . The adjustment shown in Equation 4 can vary up to  $1.2^\circ\text{C}$  between locations with  $SVF = 0.1$  and  $SVF = 0.33$ .

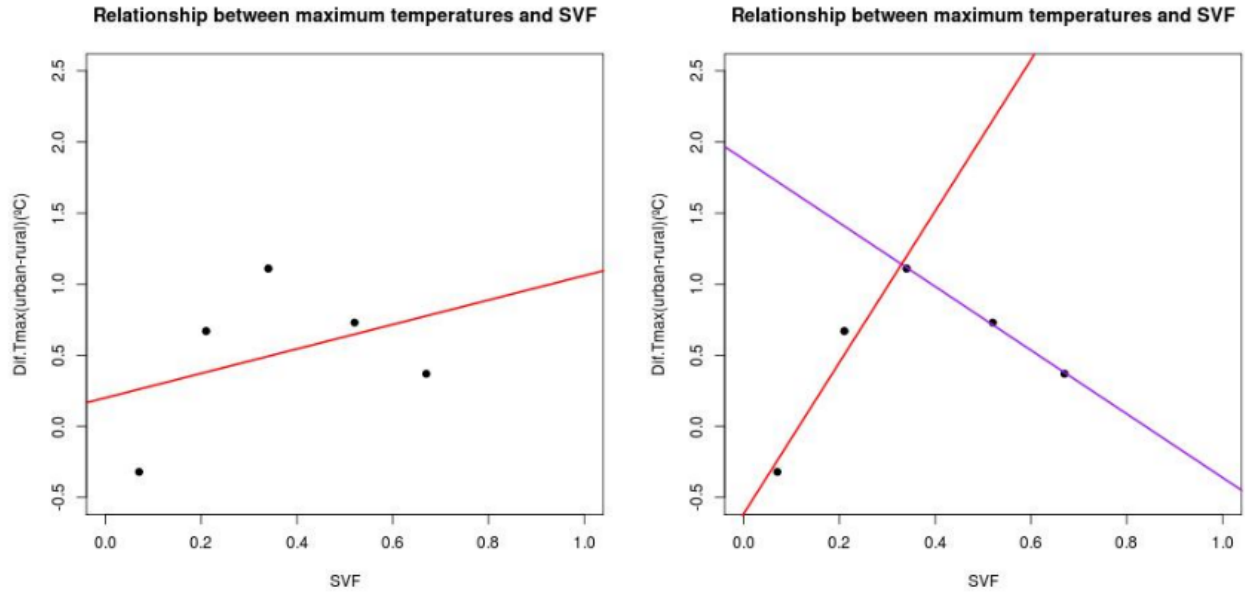


**Figure 8.** On the left, regression of the mean maximum temperature differences between each urban location and the rural area (SVF = 0.84) for SVF urban values. On the right, regression of the mean maximum temperature differences between each urban location and the rural area (SVF = 0.84) for SVF high urban values (in purple) and SVF low urban values (in red).

According to Equation 5, the wind speed at 12 UTC was the only meteorological parameter which remained in the adjustment, which confirms the proposed adjustment. The difference between a calm day and a day with a wind speed of  $20 \text{ km h}^{-1}$  reduces the  $\Delta T_{max}(\text{urban-rural})$  by more than  $1.5^\circ\text{C}$ . The adjustment can vary up to  $0.2^\circ\text{C}$  between locations with  $\text{SVF} = 0.33$  and  $\text{SVF} = 0.8$ .

These results coincide with those obtained in other research, which showed the sensitivity and rapid changes in the difference between urban and rural temperatures to changes in parameters such as cloud cover and wind speed (Gedzelman et al., 2003).

The results of the verification process of the models obtained (Equations 4 and 5) are shown in Table 4. These results were calculated using the control days, for low and high SVF values, respectively.

### 3.3 Spatial layout of urban forecasted extreme temperatures. Thermometric maps

Once the forecast models for the next day forecasted maximum and minimum temperature differences had been calculated, we could accept the next-day prediction of  $T_{min}(\text{rural})$  of Equation 3 and  $T_{max}(\text{rural})$  of Equations 4 and 5, and approximate them for the calculations  $T_{min}(\text{urban})$  and  $T_{max}(\text{urban})$ . In order to extend the prediction to any point in the city of Murcia, we calculated the SVF values in the city, according to Subsection 2.2. By the same resolution, a grid of constant values for each of the re-

maining elements of Equations 3, 4 and 5 was developed so that:

$$[T_{min}(\text{urban})]_{grid} - [T_{min}(\text{rural})] = 2.19 - 0.03[Cloud_{00}] - 1.05[SVF]_{grid} \quad (6)$$

$$\text{SVF} \leq 0.33 : [T_{max}(\text{urban})]_{grid} - [T_{max}(\text{rural})] = 0.58 - 0.04[Cloud_{12}] + 5.13[SVF]_{grid} \quad (7)$$

$$\text{SVF} \geq 0.33 : [T_{max}(\text{urban})]_{grid} - [T_{max}(\text{rural})] = 1.93 - 0.09[Wind_{12}] - 1.84[SVF]_{grid} \quad (8)$$

Using Equations 6, 7 and 8 and knowing the forecasted value for the next day maximum and minimum temperatures in the rural area, as well as the cloudiness at 00 and 12 UTC and the wind speed at 12 UTC, provided by the Ensemble Prediction System (EPS) median from ECMWF, we tried out the forecast of extreme temperatures for the next day in every point of the city of Murcia:  $[T_{min}(\text{urban})]_{grid}$ , and  $[T_{max}(\text{urban})]_{grid}$ .

In Figure 9, there is an example of the spatial layout of the calculated extreme temperatures in Murcia for a forecasted  $T_{max}(\text{rural})$  of  $38^\circ\text{C}$  and a  $T_{min}(\text{rural})$  of  $22^\circ\text{C}$ , clear skies and weak winds. These temperature values were chosen as they coincide with the thresholds outlined in the plan of preventive actions against the effects of excessive temperatures mentioned in Section 1. Table 5 indicates the extreme temperature values calculated using Equations 6, 7 and 8 in each of the urban locations pertaining to the network, as well as the recorded values at the same locations, in

**Table 5.** Values calculated using Equations 6, 7 and 8 in each of the urban locations, on a day with a maximum rural temperature of 38°C and another day with a minimum rural temperature of 22°C.

SVF	$T_{max}(urb)_{pred}$	$T_{max}(urb)_{obs}$	$T_{max(pred)} - T_{max(obs)}$	$T_{min}(urb)_{pred}$	$T_{min}(urb)_{obs}$	$T_{min(pred)} - T_{min(obs)}$
0.07	37.8	37.5	0.3	24.1	23.7	0.4
0.21	38.5	38.9	-0.4	24.0	23.5	0.5
0.34	39.3	38.4	-0.1	23.8	23.6	0.2
0.52	39.0	38.9	0.1	23.6	23.1	0.5
0.67	38.7	38.5	0.2	23.5	23.3	0.2

**Table 6.** Comparison of heat wave days defined by the Plan, in urban and rural areas, from June to September 2010.

SVF	0.84 (rural)	0.67	0.52	0.34	0.21	0.07
No. of days with $T_{max} > 38^{\circ}\text{C}$ and $T_{min} > 22^{\circ}\text{C}$	5	6	7	7	7	3
Percentage of heat wave days over 98 days (%)	5.4	6.5	7.6	7.6	7.6	3.2

the case of  $T_{max}(rural) = 38^{\circ}\text{C}$  and  $T_{min}(rural) = 22^{\circ}\text{C}$ . As shown in Table 5, the maximum urban temperatures calculated range from 37.8°C in the narrowest streets, with a low SVF value, to 39.3°C in locations with intermediate SVF values and which are more exposed to solar radiation and are poorly ventilated. Minimum temperatures ranged from 23.5°C in wider streets, with a high SVF value, to 24.1°C in narrower streets.

As shown in Subsection 3.2, the effect of SVF on the spatial distribution of extreme urban temperatures can only explain part of the variability observed, as other factors are involved here, the majority of which are of an urban nature. Despite this, the spatial distribution of the minimum urban temperatures, calculated using Equation 6 and which is demonstrated in Figure 9 (right), resembles the behaviour identified by other authors (Unger, 2004). With respect to the spatial distribution of maximum temperatures, various transects carried out during the period in question revealed positive behaviour for Equations 7 and 8 in locations with very low and very high SVF values. However, in locations with intermediate SVF values, the transects carried out showed moderate dependence between the temperature and the position of the street. Differences of more than 0.5°C were found in any one street, depending on whether the area was shaded or sunny. Differences of this type were also detected in shaded areas with the same SVF value, but given their orientation they were ventilated to a greater or lesser degree by the prevailing wind at these hours during the test period.

### 3.4 Responding to the health authorities' uncertainties

From the analysis of the recorded data, we were able to respond to the health authorities' uncertainties, mentioned in the Introduction section. During the period of the thermometric network (98 days in 2010), the specified thresholds outlined in the Plan ( $T_{max} > 38^{\circ}\text{C}$  and  $T_{min} > 22^{\circ}\text{C}$ ) were

both exceeded on the days detailed in Table 6. In accordance with Table 6, surpassing these thresholds is more likely in most of the urban locations (SVF values higher than 0.2), with the exception of shaded locations with a very low SVF value (lower than 0.1).

## 4 Conclusions

With the aim of studying the differential behaviour between rural and urban temperatures, a database of ten-minute temperatures from different locations in the city of Murcia with a wide range of SVF values was obtained.

The observed data confirmed the presence of the urban heat island (UHI) at night in the city of Murcia and its greater effect in streets with lower SVF values. Also, in these locations the opposite phenomenon, known as the urban cool island (UCI), was observed during the day.

The dependence of temperature differences between urban and rural areas with SVF was confirmed; there was a linear relationship between the SVF and the *urban-rural* mean minimum temperature differences. In the case of maximum temperatures, two linear adjustments between the *urban-rural* mean maximum temperature differences and low and high SVF values were proposed.

In order to adapt the forecast of extreme temperatures to the city, some adjustments between urban and rural observed temperature differences were worked out by means of Model Output Statistics (MOS), based on forecasted meteorological parameters and SVF. Cloudiness was a significant meteorological parameter according to the forecast model obtained for daily minimum temperature differences between urban and rural areas, but it had little influence on these differences. For daily maximum temperature differences between urban and rural areas, two forecast models for low and high SVF values were proposed. Cloudiness was the only meteorological parameter which took part in the forecast model with low



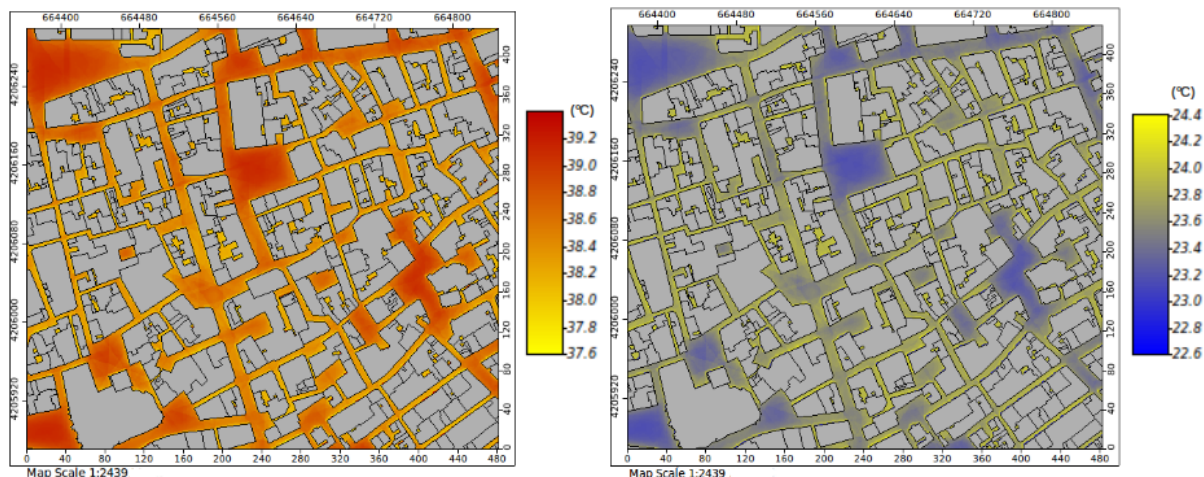


**Figure 9.** Thermometric maps obtained using Equations 6, 7 and 8 for maximum (left) and minimum (right) temperatures during a day with a maximum rural temperature of 38°C and another day with a minimum rural temperature of 22°C.

SVF values. However, wind speed was the only meteorological parameter which intervened in the forecast model with high SVF values.

Once the forecast models for the next day *urban-rural* maximum and minimum temperature differences had been calculated, the daily extreme urban forecasted temperatures were obtained for each one-meter cell size corresponding to the city of Murcia. Furthermore, some thermometric maps were obtained which showed the spatial layout of extreme temperatures in the city of Murcia.

**Acknowledgements.** We would like to thank the Ministry of Environmental, Rural and Marine Affairs for the postgraduate training grant “Spatial layout of forecasted extreme temperatures in the city of Murcia (Spain)” (Official State Journal 15/09/2008 and 23/12/2009), through which this line of research has been made possible. We would also like to recognise the participation and dedication of the staff at the AEMET Regional Office in Murcia, where this research was carried out. Furthermore, we would like to thank Murcia City Council for its support.

## References

- Becker, R. A., Chambers, J. M., and Wilks, A. R., 1988: The new S language. A programming environment for data analysis and graphics. Wadsworth & Brooks, Cole Advanced Books & Software, Pacific Grove, CA.
- Cuadrat, J. M., Vicente-Serrano, S. M., and Saz, M. A., 2005: *Los efectos de la urbanización en el clima de Zaragoza (España): estudio de la isla de calor y de sus factores condicionantes*, Boletín de la A.G.E., **40**, 311–327.
- de Steffens, A. C., Piccolo, M. C., González, J. H., and Navarrete, G., 2001: *La isla de calor estival en Temuco, Chile*, Pap geogr, **33**, 49–60.
- Eliasson, I., 1996: *Intra-urban nocturnal temperature differences: a multivariate approach*, Clim Res, **7**.

- Fernández, F., Montávez, J. P., González-Rouco, J. F., and Valero, F., 2004: *Relación entre la estructura espacial de la isla térmica y la morfología urbana de Madrid*, El clima, entre el mar y la montaña. Publicaciones de la Asociación Española de Climatología (AEC) serie A, **4**, 641–650.
- Fortuniak, 2008: *Numerical estimation of the effective albedo of an urban canyon*, Theor Appl Climatol, **91**, 245–258.
- Gedzelman, S. D., Austin, S., Cermak, R., Stefano, N., Partridge, S., Quesenberry, S., and Robinson, D. A., 2003: *Mesoscale aspects of the urban heat island around New York City*, Theor Appl Climatol, **75**, 29–42.
- Glahn, H. R. and Lowry, A. D., 1972: *The use of model output statistics (MOS) in objective weather forecasting*, J Appl Meteor, **11**, 1203–1211.
- Lindberg, F., Eliasson, I., and Holmer, B., 2003: Urban geometry and temperature variations, Proc. 5th Int Conf Urban Climate, p. 205–208.
- López-Gómez, A., López-Gómez, J., Fernández, F., and Arroyo, F., 1991: El clima urbano de Madrid: la isla de calor, Centro de Investigaciones sobre la Economía, la Sociedad y el Medio, CSIC, Madrid.
- Oke, T. R., 1988: Boundary layer climates, Routledge.
- Oke, T. R., 2004: Initial guidance to obtain representative meteorological observations at urban sites, World Meteorological Organization Geneva.
- Oke, T. R., 2007: *Canyon geometry and the nocturnal urban heat island: comparison of scale model and field observations*, J Climatol, **1**, 237–254.
- Oke, T. R., Johnson, G. T., Steyn, D. G., and Watson, I. D., 1991: *Simulation of surface urban heat islands under ‘ideal’ conditions at night Part 2: Diagnosis of causation*, Bound-Layer Meteor, **56**, 339–358.
- Olaya, V., 2004: A gentle introduction to SAGA GIS, The SAGA User Group eV, Gottingen, Germany, 208.
- Orden PRE/1518/2004, 2004: Orden PRE/1518/2004 de 28 de mayo, por la que se crea la Comisión Interministerial para la aplicación efectiva del Plan Nacional de actuaciones preventivas de los efectos del exceso de temperaturas sobre la salud, Ministerio

de la Presidencia, Gobierno de España.

- Robine, J. M., Cheung, S. L., Le Roy, S., Van Oyen, H., and Herrmann, F. R., 2007: *Report on excess mortality in Europe during summer 2003*, EU Community Action Programme for Public Health, Grant Agreement, **2005114**, 28.
- Souza, L. C. L., Rodrigues, D. S., and Mendes, J. F. G., 2003: Sky view factors estimation using a 3D-GIS extension, International Building Performance Simulation Association.
- Steyn, D. G., 1980: The calculation of view factors from fisheye-lens photographs: Research note, Taylor & Francis.
- Unger, J., 2004: *Intra-urban relationship between surface geometry and urban heat island: review and new approach*, Climate Res, **27**, 253–264.
- Unger, J., 2009: *Connection between urban heat island and sky view factor approximated by a software tool on a 3D urban database*, Int J Environ Pollut, **36**, 59–80.
- WMO, 2007: WMO to provide guidance for heat health warning systems, World Meteorology Organization, Press Release No. 781.